INTERNATIONAL JOURNAL FOR NUMERICAL METHODS IN FLUIDS
Int. J. Numer. Meth. Fluids 2009; **59**:259–284
Published online 21 February 2007 in Wiley InterScience (www.interscience.wiley.com). DOI: 10.1002/fld.1456

A posteriori estimators for vertex centred finite volume discretization of a convection–diffusion-reaction equation arising in flow in porous media

B. Amaziane[1,*,†], A. Bergam[2], M. El Ossmani[1] and Z. Mghazli[2]

[1] *Université de Pau, Laboratoire de Mathématiques Appliquées, CNRS-UMR5142, Av. de l'Université, 64000 Pau, France*
[2] *Université Ibn Tofaïl, Faculté des Sciences, Equipe d'Ingénierie Mathématique (E.I.MA.), B.133 Kénitra, Marocco*

SUMMARY

We present an adaptive numerical technique for solving convection–diffusion-reaction problems, modelling the transport of contaminant in porous media. We develop and analyse residual error estimators using finite volume approximations. The error estimators with respect to both time and space yield global upper and local lower bounds on the error measured in the energy norm. Computational results of various model simulations of fluid flow and transport of contaminant in heterogeneous aquifers are presented and discussed. Copyright © 2007 John Wiley & Sons, Ltd.

Received 10 May 2006; Revised 4 December 2006; Accepted 29 December 2006

KEY WORDS: finite volume; *a posteriori* error estimation; adaptive method; convection–diffusion-reaction equation

1. INTRODUCTION

We aim to develop, analyse, implement, and test a computational self-adaptive technique for simulation of fluid flow and transport of contaminant in porous media. We consider the concentration equation describing miscible flow in heterogeneous porous media. The solutions of these problems can involve multiple time and spatial scales, long simulation time periods, and many

*Correspondence to: B. Amaziane, Université de Pau, Laboratoire de Mathématiques Appliquées, CNRS-UMR5142, Av. de l'Université, Pau F-64000, France.
†E-mail: brahim.amaziane@univ-pau.fr

Contract/grant sponsor: CNRS ANDRA BGRM CEA EDF IRSN
Contract/grant sponsor: CMIMF Actions Intégrées; contract/grant numbers: *MA*/02/34, *MA*/04/94

coupled components which are convection dominated. The latter requires steep gradients to be preserved with minimal oscillation and numerical diffusion. Thus, dynamic time and spatial adaptivity based on *a posteriori* error estimates is essential for accuracy and efficiency. Here, we develop a computational technique that utilizes finite volume (FV) approximation of the differential equation and *a posteriori* error estimators that will lead to adaptive local grid refinement.

FV methods are a class of discretization schemes that have proved to be highly successful in approximating the solution of a wide variety of conservation laws systems. There is an extensive literature on this subject. We will not attempt a literature review here, but merely mention a few references. They are extensively used in fluid mechanics, meteorology, electromagnetics, semiconductor device simulation, models of biological processes and many other engineering areas governed by conservative systems that can be written in integral control volume form (see, e.g. [1–7]). The primary advantages of these methods are numerical robustness through the obtaining of discrete maximum principles, applicability on very general unstructured meshes, and the intrinsic local conservation properties of the resulting schemes.

The literature associated with the foundation and analysis of the FV methods for hyperbolic problems is extensive (see, e.g. [2, 6] and the references therein). FV methods for elliptic problems have been proposed and analysed under a variety of different names: box methods, covolume methods, diamond cell methods, integral finite difference methods and FV element methods (see, e.g. [7] for a review).

More recently, FV methods were developed and analysed for convection–diffusion problems (see, for instance [2, 3, 8–17]). There are various approaches in deriving FV approximations of convection–diffusion equations. The most general classification is obtained depending on the choice of: (1) the FVs and (2) the discrete space to which the approximate solution belongs. The domain is meshed and depending on whether the FVs are the elements from the original splitting or volumes around the vertices of the original splitting, we have correspondingly cell-centred and vertex-centred FV methods. For the vertex-centred FVs, depending on whether the discrete space is piecewise constant over the FVs or piecewise linear over the original mesh, we have correspondingly vertex-centred FV difference methods or vertex-centred FV element methods. The cell-centred FV can lead to cell-centred FV difference methods or mixed methods.

In this paper we construct, theoretically justify, and test a computational method that yields reliable error control of the FV discretization of a convection–diffusion-reaction equation, arising from the modelling of flow and transport in porous media, in 2-D on unstructured grids. A detailed description of the model is given by Bear and Bachmat [18]. We achieve balance between obtaining reliable control of the error and efficient use of the available computational resources by an adaptive process of local grid refinement based on *a posteriori* error analysis.

There is an extensive literature on adaptive methods for finite element approximations with emphasis on both theoretical and computational aspects of the methods. Among the wide literature we refer, e.g. to [19, 20]. There are few works related to *a posteriori* error estimates for FV methods of convection–diffusion problems. Earlier results related to this topic in the context of flow and transport in porous media were published in [4, 8, 12, 16, 21] and the references therein. Let us also mention that *a posteriori* error analysis for a linear and nonlinear elliptic problem approximated by a vertex-centred scheme were presented in [22–24].

In this paper, we introduce two kinds of indicators, both of them of residual type. The first one is related to time discretization and is local with respect to the time discretization: thus, at each time, it provides an appropriate information for the choice of the next time step. The second is related to space discretization and is local with respect to both the time and space variable and the

DOI: 10.1002/fld

idea is that at each time it is an efficient tool for mesh adaptivity. Here, we develop and analyse a fully discretized approach as in [25, 26] for finite element methods.

The paper is organized as follows. In Section 2 all necessary mathematical notations are defined, the problem is formulated and the general assumptions are stated. In Section 3, the numerical scheme for the model problem is presented with emphasis on the FV method employed for the solution of the convection–diffusion-reaction equation. The construction of error indicators for this approximation and the proof of upper and lower bounds for the error as a function of the indicators are established in Section 4. A series of numerical examples demonstrates the efficiency of the methodology for 2-D miscible flow problems through heterogeneous porous media where large permeability variations are allowed.

2. STATEMENT OF THE PROBLEM AND ASSUMPTIONS

We consider the following convection–diffusion-reaction problem: Find $u=u(x,t)$ such that

$$\begin{aligned} \frac{\partial u}{\partial t} - \operatorname{div}(D(x,t)\nabla u - \mathbf{q}u) + au = f &\quad \text{in } \Omega\times]0,T[\\ u = 0 &\quad \text{on } \Gamma\times]0,T[\\ u(\cdot,0) = u_0 &\quad \text{in } \Omega \end{aligned} \tag{1}$$

Here, Ω is a bounded polygonal domain in $\mathbb{R}^2$, with Lipschitz boundary Γ and $]0,T[$ a time interval, D is a uniformly positive function in $\bar{\Omega}\times]0,T[$, $\mathbf{q}$ is a given vector function (velocity), a is a given reaction coefficient, and f is a given source term. For simplicity we have considered a homogeneous Dirichlet boundary condition but it is easy to see that all the results are valid for other boundary conditions.

In what follows we use standard notations for Sobolev spaces. Let us state the following assumptions.

(A1) D is a positive and continuously time-differentiable function such that

$$\forall x\in\bar{\Omega}, \forall t\in]0,T[, \quad 0<D_{\min}\leqslant D(x,t)\leqslant D_{\max}<+\infty$$

Here we consider, for the analysis of the method, that the dispersion D reduces to a scalar function. However, the implementation is based on a realistic case where D is a positive definite symmetric tensor.

(A2) $f\in L^2(0,T;L^2(\Omega))$
(A3) $\mathbf{q}\in C(0,T;(W^{1,\infty}(\Omega))^2)$
(A4) $a\in C(0,T;L^{\infty}(\Omega))$
(A5) There are two constant $\beta\geqslant 0$ and $\mathscr{A}\geqslant 0$ such that

$$\tfrac{1}{2}\operatorname{div}\mathbf{q} + a \geqslant \beta \quad \text{and} \quad \|a\|_{L^{\infty}(\Omega)}\leqslant \mathscr{A}\beta \quad \text{in } [0,T]$$

(A6) $u_0\in H^1(\Omega)$.

The space $H_0^1(\Omega)$ will be equipped with the energy norm

$$|\!|\!| v |\!|\!| = (\|D^{1/2}\nabla v\|_{0,\Omega}^2 + \beta\|v\|_{0,\Omega}^2)^{1/2} \tag{2}$$

DOI: 10.1002/fld

We denote the dual norm associated to (2) by

$$|||\phi|||_* = \sup_{v\in H_0^1(\Omega), v\neq 0} \frac{\langle \phi, v\rangle}{|||v|||}, \quad \forall \phi \in H^{-1}(\Omega) \tag{3}$$

For $v\in L^2(0,T;H_0^1(\Omega))$ we introduce the norm, for all $t\in[0,T]$:

$$[[v]](t) = \left(\|v(t)\|_{0,\Omega}^2 + \int_0^t |||v(s)|||^2 \,\mathrm{d}s \right)^{1/2} \tag{4}$$

We consider the following standard weak formulation of problem (1):

$$\text{Find } u\in L^2(0,T;H_0^1(\Omega)) \text{ such that } \frac{\partial u}{\partial t} \in L^2(0,T;H^{-1}(\Omega)) \text{ and}$$

$$\begin{aligned} &\int_\Omega \frac{\partial u}{\partial t} v\,\mathrm{d}x + \int_\Omega D\nabla u\cdot\nabla v\,\mathrm{d}x + \int_\Omega \operatorname{div}(\mathbf{q}u)v\,\mathrm{d}x + \int_\Omega auv\,\mathrm{d}x \\ &\quad = \int_\Omega fv\,\mathrm{d}x \quad \forall v\in H_0^1(\Omega) \quad \text{for a.e. } t\in]0,T[\\ &u(\cdot,0) = u_0 \end{aligned} \tag{5}$$

Assumptions (A1)–(A6) imply that this problem admits a unique solution (cf. [27]), and by taking v equal to $u(t)$ in (5) and integrating on the interval $]0,t[$, we derive the following estimate, for all t in $[0,T]$:

$$[[u]](t) \leqslant \left(\|u_0\|_{0,\Omega}^2 + \frac{1}{D_{\min}} \|f\|_{L^2(0,t;H^{-1}(\Omega))}^2 \right)^{1/2} \tag{6}$$

or

$$[[u]](t) \leqslant \left(\|u_0\|_{0,\Omega}^2 + \frac{1}{\beta} \|f\|_{L^2(0,t;L^2(\Omega))}^2 \right)^{1/2} \tag{7}$$

In the case where $a\equiv 0$, i.e. no reaction term in the equation, we take $\mathscr{A}=0$ and we keep β in the definition of the energy norm.

3. DISCRETIZATION OF THE PROBLEM

Before describing the FV discretization of the model problem (1), we give some notation. We introduce a partition of the interval $[0,T]$ into subintervals $[t_{n-1},t_n]$, $1\leqslant n\leqslant N$ such that $0=t_0<t_1<\cdots<t_N=T$. We denote by τ_n the length t_n-t_{n-1}, by τ the N-uplet $(\tau_1,\ldots,\tau_N)$ and by $|\tau|$ the maximum of the τ_n, $1\leqslant n\leqslant N$. Since our aim is mesh adaptivity, for each n, $0\leqslant n\leqslant N$, we consider $(\mathscr{T}_h^n)_h$ a regular triangulation of Ω by closed triangles. Each triangulation $\mathscr{T}_h^n$ is derived from $\mathscr{T}_h^{n-1}$ by cutting some elements of $\mathscr{T}_h^{n-1}$ into a few subelements or, by the opposite i.e. gluing together some elements of $\mathscr{T}_h^{n-1}$ into a new triangle. We denote also by $\mathscr{V}_h^n$ the dual decomposition associated to $\mathscr{T}_h^n$. Note that at the same time t_n, several triangulations can

DOI: 10.1002/fld

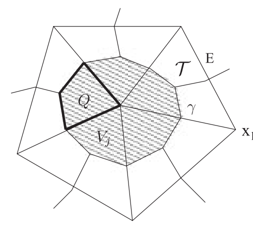

Figure 1. A vertex-centred cell in 2-D.

be employed for mesh adaptivity and we use the notation $\mathscr{T}_h^n$ only for the last one. Furthermore, let us denote $u^n = u(t_n)$, $D^n = D(t_n)$, $a^n = a(t_n)$ and $f^n = f(t_n)$.

We consider the following semi-implicit time discretization of problem (1):

$$\frac{u^n - u^{n-1}}{\tau_n} - \operatorname{div}(D^n \nabla u^n - \mathbf{q}^{n-1} u^{n-1}) + a^n u^n = f^n \quad \text{in } \Omega \tag{8}$$

We now describe the space discretization with a FV scheme. Let us give the assumptions which are needed on the mesh. Assume that we have a family of triangulations $\mathscr{T}_h^n$, which is regular (see [28]). The partition $\mathscr{V}_h^n$ is chosen as the set of N_n volumes V_i that constitute the dual of the triangulation $\mathscr{T}_h^n$ known as the Voronoi mesh and such that $\bar{\Omega} = \bigcup_{i=1,\ldots,N_n} V_i$. This mesh is constructed by connecting the middle points of edges and circumcentres of each neighbouring pair of triangles having a common edge with a straight line segment (see Figure 1).

We denote by $\mathscr{E}_h^n$ the set of edges E of triangulation $\mathscr{T}_h^n$, $h>0$ and Γ_h^n the set of edges γ of the dual decomposition $\mathscr{V}_h^n$. We denote by γ_{ij} the intersection of boundary ∂V_i and ∂V_j of two control volumes.

We may construct another partition of Ω, denoted by $\mathscr{Q}_h^n$ and formed by quadrilaterals Q defined by $Q = V \cap \mathscr{T}$ where $V \in \mathscr{V}_h^n$ and $T \in \mathscr{T}_h^n$. We also need to define the set $\mathscr{K}_h^i = \bigcup K$, formed by the triangles K having x_{V_i} (the centre of the control volume V_i) as a vertex and γ as an edge. Next, we define the spaces $\mathscr{P}_1(\mathscr{T}_h^n)$ and $\mathscr{P}_0(\mathscr{V}_h^n)$ by

$$\mathscr{P}_1(\mathscr{T}_h^n) = \{v_h \in C^0(\bar{\Omega}) : v_h|_{\mathscr{T}} \in \mathscr{P}_1; \forall \mathscr{T} \in \mathscr{T}_h^n\}$$

and

$$\mathscr{P}_0(\mathscr{V}_h^n) = \{w_h \in L^2(\bar{\Omega}) : w_h|_{V_i} \in \mathscr{P}_0; i = 1, \ldots, N_n\}$$

where $\mathscr{P}_\mathrm{l}$ is the set of polynomial functions of degree $\leqslant l$. Let $(\psi_i)_{i=1,\ldots,N_n}$ be the set of basis functions of $\mathscr{P}_1(\mathscr{T}_h^n)$.

Denote by $I_m : L^2(\Omega) \longrightarrow \mathscr{P}_0(\mathscr{V}_h^n)$ the global $\mathscr{V}_h^n$-piecewise constant interpolation operator which is defined by

$$I_m v := \begin{cases} \dfrac{1}{|V|} \displaystyle\int_V v \, \mathrm{d}x & \text{for interior volume } V \\ 0 & \text{for boundary volume } V (\text{i.e. } \partial V \cap \Gamma \neq \emptyset) \end{cases} \tag{9}$$

Note that the operator I_m satisfies homogeneous Dirichlet boundary conditions, i.e. $I_m v = 0$ on Γ.

DOI: 10.1002/fld

Integrating the semi-discrete problem (8) over a control volume V_i, we get

$$\int_{V_i} \frac{u^n - u^{n-1}}{\tau_n}\,\mathrm{d}x - \sum_{\gamma\subset\partial V_i}\left\{\int_\gamma D^n \nabla u^n\cdot \mathbf{n}_\gamma\,\mathrm{d}s - \int_\gamma \mathbf{q}^{n-1}u^{n-1}\cdot\mathbf{n}_\gamma\,\mathrm{d}s\right\} + \int_{V_i} a^n u^n\,\mathrm{d}x = \int_{V_i} f^n\,\mathrm{d}x \tag{10}$$

where $\mathbf{n}_\gamma$ is the unit outward normal vector on γ.

Equation (10) could be written in the following form:

$$\int_{V_i} \frac{u^n - u^{n-1}}{\tau_n}\,\mathrm{d}x - \sum_{\gamma\subset\partial V_i}(\mathscr{F}(u^n,\gamma) - \mathscr{G}(u^{n-1},\gamma)) + \int_{V_i} a^n u^n\,\mathrm{d}x = \int_{V_i} f^n\,\mathrm{d}x$$

where

$$\mathscr{F}(v,\gamma) := \int_\gamma D\nabla v\cdot\mathbf{n}_\gamma\,\mathrm{d}s$$

and

$$\mathscr{G}(v,\gamma) := \int_\gamma \mathbf{q}v\cdot\mathbf{n}_\gamma\,\mathrm{d}s$$

The FV discretization is ended by defining a numerical flux functions $\mathscr{F}_h(v_h^n,\gamma)$ and $\mathscr{G}_h(v_h^{n-1},\gamma)$. For this, we will consider V_h the space of all continuous, piecewise linear finite element functions corresponding to $\mathscr{T}_h^n$ and vanishing on Γ:

$$V_h := \{v_h \in \mathscr{P}_1(\mathscr{T}_h^n) \text{ and } v_h|_\Gamma = 0\} \tag{11}$$

Let M_n be the number of interior vertex. For $u_h = \sum_{i=1}^{M_n} u_i\psi_i$, the numerical flux functions $\mathscr{F}_h(u_h^n,\gamma)$ and $\mathscr{G}_h^{n-1}(u_h,\gamma)$ are defined by

$$\mathscr{F}_h(u_h^n,\gamma) = \sum_{j\in\mathscr{J}(i),\gamma=\gamma_{ij}} \int_{\gamma_{ij}} D_h^n\nabla u_h^n\cdot\mathbf{n}_\gamma\,\mathrm{d}s$$

and

$$\mathscr{G}_h(u_h^{n-1},\gamma) = \sum_{j\in\mathscr{J}(i),\gamma=\gamma_{ij}} \int_{\gamma_{ij}} ((\mathbf{q}^{n-1}\cdot\mathbf{n}_{\gamma_{ij}})^+ u_h^{n-1}(x_i) + (\mathbf{q}^{n-1}\cdot\mathbf{n}_{\gamma_{ij}})^- u_h^{n-1}(x_j))\,\mathrm{d}s$$

where

$$\mathscr{J}(i) = \{j\in\{1,\ldots,M_n\} : \operatorname{supp}\psi_i \cap \operatorname{supp}\psi_j \neq \emptyset\}$$

$$(\mathbf{q}^{n-1}\cdot\mathbf{n})^+ = \max(0,\mathbf{q}^{n-1}\cdot\mathbf{n}),\quad (\mathbf{q}^{n-1}\cdot\mathbf{n})^- = \min(0,\mathbf{q}^{n-1}\cdot\mathbf{n})$$

and D_h^n is an approximation of $D(t_n)$ which is a piecewise polynomial of degree smaller than a fixed integer ℓ and such that there exists a constant $c(D)$ only depending on D satisfying

$$\|D(t_n) - D_h^n\|_{L^\infty(\Omega)} \leqslant c(D)h^{\ell+1},\quad 1\leqslant n\leqslant N \tag{12}$$

DOI: 10.1002/fld

We assume that a_h^n is also an approximation of $a(t_n)$ which is piecewise polynomial of degree smaller than a fixed integer ℓ and such that there exists a constant $c(a)$ only depending on a satisfying

$$\|a(t_n) - a_h^n\|_{L^\infty(\Omega)} \leqslant c(a)h^{\ell+1}, \quad 1 \leqslant n \leqslant N \tag{13}$$

The fully discrete problem is then given by

$$\begin{aligned}
&\text{Find } (u_h^n)_{0\leqslant n\leqslant N} \in (V_h)^{N+1} \text{ satisfying}\\
&u_h^0 = \Pi_h u_0 \quad \text{in } \Omega\\
&\int_{V_i^n} \frac{u_h^n - u_h^{n-1}}{\tau_n}\,\mathrm{d}x - \sum_{j\in\mathscr{I}(i)} \int_{\gamma_{ij}} (D_h^n \nabla u_h^n \cdot \mathbf{n}_{\gamma_{ij}}\\
&\quad -[(\mathbf{q}^{n-1}\cdot\mathbf{n}_{\gamma_{ij}})^+ u_h^{n-1}(x_i) + (\mathbf{q}^{n-1}\cdot\mathbf{n}_{\gamma_{ij}})^- u_h^{n-1}(x_j)])\,\mathrm{d}s\\
&\quad +\int_{V_i^n} a_h^n u_h^n\,\mathrm{d}x = \int_{V_i^n} f^n\,\mathrm{d}x\\
&\text{for } i = 1, 2, \ldots, M_n, \quad n = 1, \ldots, N
\end{aligned} \tag{14}$$

where V_i^n for $1 \leqslant i \leqslant M_n$, are the interior control volumes in $\mathscr{V}_h^n$, a_h^n is a piecewise linear approximation of a^n and Π_h is the L^2-projection on V_h.

The analysis and numerical results of this scheme applied to immiscible and miscible flow in porous media can be found in [29, 30] and [31, 32], respectively.

Remark 3.1

The terms $\int_{V_i}((u^n - u^{n-1})/\tau_n)\,\mathrm{d}x$ and $\int_{V_i} a^n u^n\,\mathrm{d}x$ could be approximated by $|V_i|((u_i^n - u_i^{n-1})/\tau_n)$ and $|V_i| a_i^n u_i^n$, respectively, where $u_i^n = u_h^n(x_i)$ and $a_i^n = a_h^n(x_i)$.

With the family $(u_h^n)_{0\leqslant n\leqslant N}$ we associate the function $u_{h\tau}$ on $[0, T]$ which is linear on each interval $[t_{n-1}, t_n]$, $1 \leqslant n \leqslant N$, and equal to u_h^n at t_n, for $0 \leqslant n \leqslant N$. This function writes, for $1 \leqslant n \leqslant N$

$$u_{h\tau}(t) = u_h^n - \frac{t_n - t}{\tau_n}(u_h^n - u_h^{n-1}) \quad \forall t \in [t_{n-1}, t_n] \tag{15}$$

$$u_{h\tau}(t) = u_h^{n-1} + \frac{t - t_{n-1}}{\tau_n}(u_h^n - u_h^{n-1}) \quad \forall t \in [t_{n-1}, t_n] \tag{16}$$

4. *A POSTERIORI* ERROR ESTIMATES

In this section, we derive an adaptive numerical technique using the FV approximation described in the previous section. The method expresses the error in terms of the residual of the approximate solution. For this, we will bound the norms of $[[u - u_{h\tau}]](t_n)$, for $1 \leqslant n \leqslant N$, as a function of indicators.

DOI: 10.1002/fld

Let us define the residuals and inter-element jumps of the approximation $(u_h^n)_n$:

$$\mathbf{R_h^n}|_Q := \left(f_h^n - \frac{u_h^n - u_h^{n-1}}{\tau_n} + \operatorname{div}(D_h^n \nabla u_h^n) - \operatorname{div}(\mathbf{q}^{n-1} u_h^{n-1}) - a_h^n u_h^n \right) \tag{17}$$

$$\mathbf{r_h^n}|_E := [D_h^n \nabla u_h^n \cdot \mathbf{n}_E] \tag{18}$$

$$\mathbf{z_h^n}|_\gamma := \mathbf{q}^{n-1} \cdot \bar{\mathbf{n}}_\gamma (u_h^{n-1}(x_i) - u_h^{n-1}(x)) \tag{19}$$

where [.] denotes as usual the jump across the edge E.

The local spatial error indicators are defined by

$$(\eta_{\mathbf{R}}^n)^2 := \sum_{V \in \mathscr{T}^*} \sum_{Q \subset V} \alpha_Q^2 \|\mathbf{R_h^n}\|_{0,Q}^2 \tag{20}$$

$$(\eta_{\mathbf{r}}^n)^2 := D_{\min}^{-1/2} \sum_{E \in \mathscr{E}} \alpha_E \|\mathbf{r_h^n}\|_{0,E}^2 \tag{21}$$

$$(\eta_{\mathbf{z}}^n)^2 := D_{\min}^{-1/2} \sum_{\gamma \in \Gamma_h^n} \alpha_\gamma \|\mathbf{z_h^n}\|_{0,\gamma}^2 \tag{22}$$

where $\alpha_S := \min(h_S D_{\min}^{-1/2}, \beta^{-1/2})$ for $S = K, E, \gamma$.

Finally the global spatial error indicator is given by

$$(\eta_h^n)^2 := (\eta_{\mathbf{R}}^n)^2 + (\eta_{\mathbf{r}}^n)^2 + (\eta_{\mathbf{z}}^n)^2 \tag{23}$$

We define the temporal error indicator as

$$\begin{aligned}\mathbf{\Theta_h^n} := \Big[\frac{\tau_n}{3} (&\|(D_h^n)^{1/2} \nabla (u_h^n - u_h^{n-1})\|^2 + \|\operatorname{div}(\mathbf{q}^{n-1}(u_h^{n-1} - u_h^n))\|^2 \\ &+ \|(a_h^n)^{1/2}(u_h^n - u_h^{n-1})\|^2) \Big]^{1/2}\end{aligned} \tag{24}$$

and the indicator related to data by

$$\begin{aligned}\mathbf{G_h^n}(t) := \max(\beta^{-1/2}, D_{\min}^{-1/2})(&\|f - f_h^n + \operatorname{div}((\mathbf{q}^{n-1} - \mathbf{q}) u_{h\tau}) + (a_h^n - a) u_{h\tau}\|_0 \\ &+ \|(D_h^n - D) \nabla u_{h\tau}\|_0)\end{aligned} \tag{25}$$

4.1. An upper bound for the error

In this subsection we will state an upper bound for the error. The following result holds:

Theorem 4.1

Let u be the solution of problem (5) and $(u_h^n)_{n \geqslant 1}$ the solution of problem (14), then there exists a constant C independent of h, such that

$$[[u - u_{h\tau}]](t_n) \leqslant C \left[\|u^0 - \Pi_0 u^0\|_0^2 + \sum_{m=1}^n \left((\eta_h^m)^2 \tau_m + (\mathbf{\Theta_h^m})^2 + \int_{t_{m-1}}^{t_m} |\mathbf{G_h^n}(t)|^2 \right) \right]^{1/2} \tag{26}$$

where η_h^m, $\mathbf{\Theta_h^m}$ and $\mathbf{G_h^n}$ are defined by (23)–(25), respectively.

DOI: 10.1002/fld

Proof
For all $v \in H_0^1(\Omega)$ we have

$$\int_\Omega \frac{\partial}{\partial t}(u-u_{h\tau})v\,\mathrm{d}x + \int_\Omega D\nabla(u-u_{h\tau})\cdot\nabla v\,\mathrm{d}x$$

$$+\int_\Omega \mathrm{div}(\mathbf{q}(u-u_{h\tau}))v\,\mathrm{d}x + \int_\Omega a(u-u_{h\tau})v\,\mathrm{d}x$$

$$=\int_\Omega (f-f_h^n)v\,\mathrm{d}x + \int_\Omega f_h^n v\,\mathrm{d}x - \int_\Omega \frac{u_h^n-u_h^{n-1}}{\tau_n}v\,\mathrm{d}x - \int_\Omega D_h^n\nabla u_h^n\cdot\nabla v\,\mathrm{d}x$$

$$+\int_\Omega D_h^n\nabla(u_h^n-u_{h\tau})\cdot\nabla v\,\mathrm{d}x + \int_\Omega (D_h^n-D)\nabla u_{h\tau}\cdot\nabla v\,\mathrm{d}x$$

$$-\int_\Omega \mathrm{div}(\mathbf{q}^{n-1}u_h^{n-1})v\,\mathrm{d}x + \int_\Omega \mathrm{div}(\mathbf{q}^{n-1}(u_h^{n-1}-u_{h\tau}))v\,\mathrm{d}x$$

$$+\int_\Omega \mathrm{div}((\mathbf{q}^{n-1}-\mathbf{q})u_{h\tau})v\,\mathrm{d}x - \int_\Omega a_h^n u_h^n v\,\mathrm{d}x$$

$$+\int_\Omega a_h^n(u_h^n-u_{h\tau})v\,\mathrm{d}x + \int_\Omega (a_h^n-a)u_{h\tau}v\,\mathrm{d}x \tag{27}$$

For all $v \in H_0^1(\Omega)$ we denote by

$$\begin{aligned}
A(v) &:= \int_\Omega f_h^n v\,\mathrm{d}x - \int_\Omega \frac{u_h^n-u_h^{n-1}}{\tau_n}v\,\mathrm{d}x - \int_\Omega D_h^n\nabla u_h^n\cdot\nabla v\,\mathrm{d}x\\
&\quad -\int_\Omega \mathrm{div}(\mathbf{q}^{n-1}u_h^{n-1})v\,\mathrm{d}x - \int_\Omega a_h^n u_h^n v\,\mathrm{d}x\\
B(v) &:= \int_\Omega D_h^n\nabla(u_h^n-u_{h\tau})\cdot\nabla v\,\mathrm{d}x + \int_\Omega \mathrm{div}(\mathbf{q}^{n-1}(u_h^{n-1}-u_{h\tau}))v\,\mathrm{d}x\\
&\quad +\int_\Omega a_h^n(u_h^n-u_{h\tau})v\,\mathrm{d}x\\
C(v) &:= \int_\Omega (f-f_h^n)v\,\mathrm{d}x + \int_\Omega (D_h^n-D)\nabla u_{h\tau}\cdot\nabla v\,\mathrm{d}x + \int_\Omega \mathrm{div}((\mathbf{q}^{n-1}-\mathbf{q})u_{h\tau})v\,\mathrm{d}x\\
&\quad +\int_\Omega (a_h^n-a)u_{h\tau}v\,\mathrm{d}x
\end{aligned} \tag{28}$$

and evaluate separately each term $A(v)$, $B(v)$ and $C(v)$.

Evaluation of the term A:

Since $I_m v$ is piecewise constant we can write A as

$$A(v) = \sum_{V\in\mathscr{V}_h^n}\int_V \left(f_h^n v - \frac{u_h^n-u_h^{n-1}}{\tau_n}v - D_h^n\nabla u_h^n\cdot\nabla(v-I_m v) - \mathrm{div}(\mathbf{q}^{n-1}u_h^{n-1})v - a_h^n u_h^n v\right)\mathrm{d}x$$

An integration by parts gives

$$A(v)=\sum_{V\in\mathscr{V}_h^n}\left\{\sum_{Q\subset V}\int_Q\left(f_h^n v-\frac{u_h^n-u_h^{n-1}}{\tau_n}v+\operatorname{div}(D_h^n\nabla u_h^n(v-I_m v))\right.\right.$$

$$\left.\left.-\operatorname{div}(\mathbf{q}^{n-1}u_h^{n-1})v-a_h^n u_h^n v\right)\mathrm{d}x+\int_{\partial V}D_h^n\nabla u_h^n\cdot\mathbf{n}I_m v\,\mathrm{d}s\right\}$$

$$+\sum_{E\in\mathscr{E}_h^n}\int_E[D_h^n\nabla u_h^n\cdot\mathbf{n}_E](v-I_m v)\,\mathrm{d}s$$

$$=\sum_{V\in\mathscr{T}_h^n}\left\{\sum_{Q\subset V}\int_Q\left(f_h^n-\frac{u_h^n-u_h^{n-1}}{\tau_n}+\operatorname{div}(D_h^n\nabla u_h^n)\right.\right.$$

$$\left.-\operatorname{div}(\mathbf{q}^{n-1}u_h^{n-1})-a_h^n u_h^n\right)(v-I_m v)\,\mathrm{d}x$$

$$\left.+\int_{\partial V}D_h^n\nabla u_h^n\cdot\mathbf{n}I_m v\,\mathrm{d}s\right\}+\sum_{E\in\mathscr{E}_h^n}\int_E[D_h^n\nabla u_h^n\cdot\mathbf{n}_E](v-I_m v)\,\mathrm{d}s$$

$$+\sum_{V\in\mathscr{T}_h^n}\int_V\left(f_h^n-\frac{u_h^n-u_h^{n-1}}{\tau_n}-\operatorname{div}(\mathbf{q}^{n-1}u_h^{n-1})-a_h^n u_h^n\right)I_m v\,\mathrm{d}x$$

For interior volumes V, the FV discretization (14) implies that the last term is equal to

$$-\sum_{V_i\in\mathscr{T}_h^n}(I_m v)_i\left(\sum_{\gamma_{ij}\subset\partial V_i}\int_{\gamma_{ij}}(\mathbf{q}^{n-1}\cdot\mathbf{n}_{\gamma_{ij}}u_h^{n-1}(x)-(\mathbf{q}^{n-1}\cdot\mathbf{n}_{\gamma_{ij}})^+u_h^{n-1}(x_i)\right.$$

$$\left.-(\mathbf{q}^{n-1}\cdot\mathbf{n}_{\gamma_{ij}})^-u_h^{n-1}(x_j))\,\mathrm{d}s\right)$$

where $(I_m v)_i=(I_m v)_{|V_i}$, and if we take $\bar{\mathbf{n}}$ to be the normal to γ_{ij} such that $\mathbf{q}^{n-1}\cdot\bar{\mathbf{n}}\geqslant 0$ and the indices (ij) are such that $(x_i-x_j)\cdot\bar{\mathbf{n}}\leqslant 0$ the last term is equal to

$$-\sum_{\mathscr{T}\in\mathscr{T}_h^n}\sum_{\gamma_{ij}\in\Gamma_h^n,\gamma_{ij}\subset\mathscr{T}}((I_m v)_i-(I_m v)_j)\int_{\gamma_{ij}}\mathbf{q}^{n-1}\cdot\bar{\mathbf{n}}(u_h^{n-1}(x_i)-u_h^{n-1}(x))\,\mathrm{d}s$$

With the help of (17)–(19), the expression $A(v)$ writes

$$A(v)=\sum_{V\in\mathscr{V}_h^n}\sum_{Q\subset V}\int_Q\mathbf{R_h^n}(v-I_m v)\,\mathrm{d}x+\sum_{E\in\mathscr{E}_h^n}\int_E\mathbf{r_h^n}(v-I_m v)\,\mathrm{d}s$$

$$-\sum_{\mathscr{T}\in\mathscr{T}_h^n}\sum_{\gamma_{ij}\in\Gamma_h^n,\gamma_{ij}\subset\mathscr{T}}((I_m v)_i-(I_m v)_j)\int_{\gamma_{ij}}\mathbf{z_h^n}\,\mathrm{d}s \tag{29}$$

□

Now the interpolation error bounds for I_m defined by (9) is given by the following Lemma.

Lemma 4.2
Let $v \in H_0^1(\Omega)$, we have the following estimates:

$$(1)\ \|v - I_m v\|_{0,K} \leqslant c_1 \alpha_K |||v|||_{\omega_K} \quad \forall K \in \mathscr{K},\ K \subset Q \tag{30}$$

$$(2)\ \|v - I_m v\|_{0,E} \leqslant c_2 D_{\min}^{-1/4} \alpha_E^{1/2} |||v|||_{\omega_E} \quad \forall E \in \mathscr{E}_h^n \tag{31}$$

$$(3)\ \|(I_m v)_i - (I_m v)_j\|_{0,\gamma_{ij}} \leqslant c_3 D_{\min}^{-1/4} \alpha_{\gamma_{ij}}^{1/2} |||v|||_{\omega_{\gamma_{ij}}} \quad \forall \gamma_{ij} \in \Gamma_h^n \tag{32}$$

where $\alpha_S := \min(h_S D_{\min}^{-1/2}, \beta^{-1/2})$ for $S = K, E, \gamma_{ij}$, and the constants c_1, c_2 and c_3 are independent of h.

Proof
(1) Let $v \in H^1(\Omega)$, $V \in \mathscr{V}_h^n$, $K \in \mathscr{K}$, $K \subset Q$ and $E \in \mathscr{E}_h^n$. We have the standard estimations

$$\|v - I_m v\|_{0,K} \leqslant c h_K \|\nabla v\|_{\omega_K}$$

$$\|v - I_m v\|_{0,K} \leqslant c' \|v\|_K$$

Hence, we get the bound (30)

$$\|v - I_m v\|_{0,K} \leqslant c_1 \min\{h_K D_{\min}^{-1/2}, \beta^{-1/2}\} |||v|||_{\omega_K}$$

(2) In order to show the interpolation bound (31) we consider the well-known trace inequality (cf. [33]) for $w \in H^1(\mathscr{T})$, for an arbitrary $\mathscr{T} \in \mathscr{T}_h^n$

$$\|w\|_{0,E} \leqslant c(h_{\mathscr{T}}^{-1/2} \|w\|_{0,\mathscr{T}} + \|w\|_{0,\mathscr{T}}^{1/2} \|\nabla w\|_{0,\mathscr{T}}^{1/2})$$

We take $w = v - I_m v$ and restrict ourself to the small triangle $K \subset \mathscr{T}$ where we have $w \in H^1(K)$, and we use the bound (30)

$$\begin{aligned}
\|v - I_m v\|_{0,E}^2 &= \sum_{K \subset \omega_T} \|v - I_m v\|_{0,E\cap K}^2 \\
&\leqslant c \sum_{K \subset \omega_T} (h_K^{-1} \alpha_K^2 |||v|||_{\omega_T}^2 + \alpha_K |||v|||_{\omega_T} D_{\min}^{-1/2} |||v|||_{\omega_T}) \\
&\leqslant c \sum_{K \subset \omega_T} (h_K^{-1} \alpha_K^2 + D_{\min}^{-1/2} \alpha_K) |||v|||_{\omega_T}^2 \\
&\leqslant 2c \sum_{K \subset \omega_T} D_{\min}^{-1/2} \alpha_K |||v|||_{\omega_T}^2 \\
&\leqslant c_2 D_{\min}^{-1/2} \alpha_E |||v|||_{\omega_T}^2
\end{aligned}$$

(3) For the bound (32), we remark that

$$\|(I_m v)_i - (I_m v)_j\|_{0,\gamma_{ij}} \leqslant \|(I_m v)_i - v\|_{0,\gamma_{ij}} + \|v - (I_m v)_j\|_{0,\gamma_{ij}}$$

and we use the same argument as in (2). This completes the proof of Lemma 4.2 □

DOI: 10.1002/fld

One can conclude from Lemma 4.2 and (29) that

$$A(v) \leqslant \sum_{V\in\mathscr{V}_h^n}\sum_{Q\subset V}\alpha_Q\|\mathbf{R_h^n}\|_{0,Q}|||v|||_{\omega_Q}+\sum_{E\in\mathscr{E}_h^n}D_{\min}^{-1/4}\alpha_E^{1/2}\|\mathbf{r_h^n}\|_{0,E}|||v|||_{\omega_E}$$
$$+\sum_{\gamma\in\Gamma_h^n}D_{\min}^{-1/4}\alpha_\gamma^{1/2}\|\mathbf{z_h^n}\|_{0,\gamma}|||v|||_{\omega_\gamma} \tag{33}$$

where $\mathbf{R_h^n}$, $\mathbf{r_h^n}$ and $\mathbf{z_h^n}$ are defined by (17)–(19), respectively.

By using the fact that the domains ω_Q, ω_E and $\omega_{\gamma_{ij}}$ only consist of a finite number of elements that is bounded by the minimal ratio of the diameter of any element to the diameter of its largest inscribed ball, we conclude that

$$A(v)\leqslant\eta_h^n|||v|||$$

and

$$\sum_{m=1}^n\int_{t_{m-1}}^{t_m}A(v)\,\mathrm{d}t\leqslant\sum_{m=1}^n\int_{t_{m-1}}^{t_m}\eta_h^m|||v|||\,\mathrm{d}t\leqslant\sum_{m=1}^n\eta_h^m\tau_m^{1/2}\left(\int_0^{t_n}|||v|||^2\,\mathrm{d}t\right)^{1/2} \tag{34}$$

where η_h^n is given by (23).

If we use the definition of η_r^n and η_z^n without the term $D_{\min}^{-1/2}$ we obtain

$$\sum_{m=1}^n\int_{t_{m-1}}^{t_m}A(v)\,\mathrm{d}t\leqslant C_1\sum_{m=1}^n\int_{t_{m-1}}^{t_m}\eta_h^m|||v|||\,\mathrm{d}t\leqslant C_1\sum_{m=1}^n\eta_h^m\tau_m^{1/2}\left(\int_0^{t_n}|||v|||^2\,\mathrm{d}t\right)^{1/2} \tag{35}$$

where $C_1=\sup(1, D_{\min}^{-1/2})$.

Evaluation of the term B:

From (15), (16), (12) and (13) we have for $0\leqslant t\leqslant t_n$

$$\int_\Omega D_h^n\nabla(u_h^n-u_{h\tau})\cdot\nabla v\,\mathrm{d}x=\left(\frac{t_n-t}{\tau_n}\right)\int_\Omega D_h^n\nabla(u_h^n-u_h^{n-1})\cdot\nabla v\,\mathrm{d}x$$
$$\leqslant\left(\frac{t_n-t}{\tau_n}\right)C_2(D)\|(D_h^n)^{1/2}\nabla(u_h^n-u_h^{n-1})\|\,|||v|||$$

where $C_2(D)=(1+c(D)h^{\ell+1}/D_{\min}^{1/2})$.

$$\int_\Omega a_h^n(u_h^n-u_{h\tau})v\,\mathrm{d}x=\left(\frac{t_n-t}{\tau_n}\right)\int_\Omega a_h^n(u_h^n-u_h^{n-1})v\,\mathrm{d}x$$
$$\leqslant\left(\frac{t_n-t}{\tau_n}\right)c(a)\|(a_h^n)^{1/2}(u_h^n-u_h^{n-1})\|\,|||v|||$$

where $C_2(a)=(1+c(a)h^{\ell+1}/\beta^{1/2})$ and

$$\int_\Omega \mathrm{div}(\mathbf{q}^{n-1}(u_h^{n-1}-u_{h\tau}))v\,\mathrm{d}x=\left(\frac{t-t_{n-1}}{\tau_n}\right)\int_\Omega\mathrm{div}(\mathbf{q}^{n-1}(u_h^{n-1}-u_h^n))v\,\mathrm{d}x$$
$$\leqslant\left(\frac{t-t_{n-1}}{\tau_n}\right)\beta^{-1/2}\|\mathrm{div}(\mathbf{q}^{n-1}(u_h^{n-1}-u_h^n))\|\,|||v|||$$

DOI: 10.1002/fld

Let

$$\boldsymbol{\xi}_{\mathbf{h}}^{\mathbf{n}} := \left(\frac{t_n - t}{\tau_n}\right) \|(D_h^n)^{1/2}\nabla(u_h^n - u_h^{n-1})\| \tag{36}$$

$$\boldsymbol{\zeta}_{\mathbf{h}}^{\mathbf{n}} := \left(\frac{t - t_{n-1}}{\tau_n}\right) \|\mathrm{div}(\mathbf{q}^{n-1}(u_h^{n-1} - u_h^n))\| \tag{37}$$

$$\boldsymbol{\alpha}_{\mathbf{h}}^{\mathbf{n}} := \left(\frac{t_n - t}{\tau_n}\right) \|(a_h^n)^{1/2}(u_h^n - u_h^{n-1})\| \tag{38}$$

One can conclude that

$$B(v) \leqslant C_4(D, a, \beta)(\boldsymbol{\xi}_{\mathbf{h}}^{\mathbf{n}} + \boldsymbol{\zeta}_{\mathbf{h}}^{\mathbf{n}} + \boldsymbol{\alpha}_{\mathbf{h}}^{\mathbf{n}})\||v\||$$

where $C_4(D, a, \beta) = \max(C_2(D), C_3(a), \beta^{-1/2})$.

With the notation (24), we have

$$\begin{aligned}\sum_{m=1}^{n}\int_{t_{m-1}}^{t_m} B(v)\,\mathrm{d}t &\leqslant C_4(D, a, \beta)\sum_{m=1}^{n} \boldsymbol{\Theta}_{\mathbf{h}}^{\mathbf{m}}\left(\int_{t_{m-1}}^{t_m} \||v\||^2\,\mathrm{d}t\right)^{1/2}\\ &\leqslant C_4(D, a, \beta)\sum_{m=1}^{n} \boldsymbol{\Theta}_{\mathbf{h}}^{\mathbf{m}}\left(\int_{0}^{t_n} \||v\||^2\right)^{1/2}\end{aligned} \tag{39}$$

Evaluation of the term C:

$$\begin{aligned}C(v) :=& \int_\Omega (f - f_h^n + \mathrm{div}((\mathbf{q}^{n-1} - \mathbf{q})u_{h\tau}) + (a_h^n - a)u_{h\tau})v\,\mathrm{d}x\\ &+ \int_\Omega (D_h^n - D)\nabla u_{h\tau}\cdot\nabla v\,\mathrm{d}x\\ \leqslant& (\beta^{-1/2}\|f - f_h^n + \mathrm{div}((\mathbf{q}^{n-1} - \mathbf{q})u_{h\tau}) + (a_h^n - a)u_{h\tau}\|_0\\ &+ D_{\min}^{-1/2}\|(D_h^n - D)\nabla u_{h\tau}\|_0)\||v\||\end{aligned}$$

One can conclude that

$$\sum_{m=1}^{n}\int_{t_{m-1}}^{t_m} C(v) \leqslant \sum_{m=1}^{n}\left(\int_{t_{m-1}}^{t_m} |\mathbf{G}_{\mathbf{h}}^{\mathbf{n}}(t)|^2\right)^{1/2}\left(\int_0^{t_n}\||v\||^2\right)^{1/2} \tag{40}$$

where $\mathbf{G}_{\mathbf{h}}^{\mathbf{n}}$ is defined by (25).

Now we integrate (27) between 0 and t_n, we use the inequalities (35), (39), (40), we take $v = (u - u_{h\tau})(\cdot, t)$ for $0 \leqslant t \leqslant t_n$ and we use the fact that for all $v \in H_0^1(\Omega)$ we have

$$\begin{aligned}&\int_\Omega |D^{1/2}\nabla v|^2\,\mathrm{d}x + \int_\Omega \mathrm{div}(\mathbf{q}v)v\,\mathrm{d}x + \int_\Omega a|v|^2\,\mathrm{d}x\\ &= \int_\Omega |D^{1/2}\nabla v|^2\,\mathrm{d}x + \int_\Omega \left(\frac{1}{2}\mathrm{div}\,\mathbf{q} + a\right)|v|^2\,\mathrm{d}x \geqslant \||v\||^2\end{aligned}$$

to obtain (26). This completes the proof of Theorem 4.1. □

DOI: 10.1002/fld

4.2. A lower bound for the error

Global upper bounds are sufficient to obtain a numerical solution with an accuracy below a prescribed tolerance. However, local lower bounds are necessary to achieve the prescribed tolerance with a minimal number of grid-points. In this subsection we derive a lower bound for the error following the approach developed in [25, 26]. We prove separate bounds for each indicator η_h^m and $\mathbf{\Theta_h^m}$. We begin with the latter.

Proposition 4.3
There exists a constant $\mathscr{C}_1 = \mathscr{C}_1(D, \beta, \mathbf{q})$ such that

$$\mathbf{\Theta_h^n} \leqslant \mathscr{C}_1 \left[\left(\int_{t_{n-1}}^{t_n} \left\| \frac{\partial}{\partial t}(u - u_{h\tau}) \right\|_{-1,\Omega}^2 \mathrm{d}t \right)^{1/2} + \left(\int_{t_{n-1}}^{t_n} |\!|\!| u - u_{h\tau} |\!|\!|^2 \, \mathrm{d}t \right)^{1/2} \right.$$
$$\left. + \tau_n^{1/2} \eta_h^n + \left(\int_{t_{n-1}}^{t_n} |\mathbf{G_h^n}(t)|^2 \, \mathrm{d}t \right)^{1/2} \right]$$

for all $1 \leqslant n \leqslant N$.

Proof
First of all we remark that

$$\left(\frac{\tau_n}{3}\right)^{1/2} |\!|\!| u_h^n - u_h^{n-1} |\!|\!| = \left(\frac{\tau_n}{3}\right)^{1/2} [\|(D^n)^{1/2} \nabla (u_h^n - u_h^{n-1})\|^2 + \beta \|u_h^n - u_h^{n-1}\|^2]^{1/2}$$
$$\leqslant \left(\frac{\tau_n}{3}\right)^{1/2} [c(D) h^{\ell+1} \|(D_h^n)^{1/2} \nabla (u_h^n - u_h^{n-1})\|^2$$
$$+ c(a) h^{\ell+1} \|(a_h^n)^{1/2} (u_h^n - u_h^{n-1})\|^2]^{1/2}$$

So we have

$$\left(\frac{\tau_n}{3}\right)^{1/2} |\!|\!| u_h^n - u_h^{n-1} |\!|\!| \leqslant C_5 \mathbf{\Theta_h^n} \tag{41}$$

where $C_5 = h^{\ell+1} \max(c(D), c(a))$.

By (27) and (28) we have $v = u_h^n - u_h^{n-1}$

$$(\mathbf{\Theta_h^n})^2 = \int_{t_{n-1}}^{t_n} \int_\Omega \frac{\partial}{\partial t}(u - u_{h\tau}) v \, \mathrm{d}x \, \mathrm{d}t + \int_\Omega D \nabla (u - u_{h\tau}) \cdot \nabla v \, \mathrm{d}x + \int_\Omega \mathrm{div}(\mathbf{q}(u - u_{h\tau})) v \, \mathrm{d}x$$
$$+ \int_\Omega a(u - u_{h\tau}) v \, \mathrm{d}x - \int_{t_{n-1}}^{t_n} (A(u_h^n - u_h^{n-1}) + C(u_h^n - u_h^{n-1})) \, \mathrm{d}t$$
$$\leqslant \int_{t_{n-1}}^{t_n} \left(\frac{1}{D_{\min}^{1/2}} \left\| \frac{\partial}{\partial t}(u - u_{h\tau}) \right\|_* + (1 + \|\mathbf{q}\|_{(L^\infty(\Omega))^2} (\beta D_{\min})^{-1/2}) |\!|\!| u - u_{h\tau} |\!|\!| \right)$$
$$\times |\!|\!| u_h^n - u_h^{n-1} |\!|\!| \, \mathrm{d}t + \int_{t_{n-1}}^{t_n} (C_1 \eta_h^n + \mathbf{G_h^n}(t)) |\!|\!| u_h^n - u_h^{n-1} |\!|\!| \, \mathrm{d}t$$

DOI: 10.1002/fld

$$\leqslant \Bigg[\left(\int_{t_{n-1}}^{t_n} \frac{1}{D_{\min}} \left\| \frac{\partial}{\partial t}(u - u_{h\tau}) \right\|_*^2 \mathrm{d}t \right)^{1/2} + C_6 \left(\int_{t_{n-1}}^{t_n} |||u - u_{h\tau}|||^2 \, \mathrm{d}t \right)^{1/2}$$

$$+ C_1 \tau_n^{1/2} \eta_h^n + \left(\int_{t_{n-1}}^{t_n} |\mathbf{G_h^n}(t)|^2 \, \mathrm{d}t \right)^{1/2} \Bigg] \tau_h^{1/2} |||u_h^n - u_h^{n-1}|||$$

where $C_6 = 1 + \|\mathbf{q}\|_{(L^\infty(\Omega))^2} (\beta D_{\min})^{-1/2}$. We conclude by using (41)

$$\mathbf{\Theta_h^n} \leqslant \mathscr{C}_1 \Bigg[\left(\int_{t_{n-1}}^{t_n} \frac{1}{D_{\min}} \left\| \frac{\partial}{\partial t}(u - u_{h\tau}) \right\|_*^2 \mathrm{d}t \right)^{1/2} + \left(\int_{t_{n-1}}^{t_n} |||u - u_{h\tau}|||^2 \, \mathrm{d}t \right)^{1/2}$$

$$+ \tau_n^{1/2} \eta_h^n + \left(\int_{t_{n-1}}^{t_n} |\mathbf{G_h^n}(t)|^2 \, \mathrm{d}t \right)^{1/2} \Bigg]$$

where $\mathscr{C}_1 = \sqrt{3} C_5 \max(1, C_6, C_1)$. This completes the proof of Proposition 4.3 □

Proposition 4.4

There exists a constant $\mathscr{C}_2 = \mathscr{C}_2(a, D, \beta, \mathbf{q})$ such that

$$\tau_n^{1/2} \eta_h^n \leqslant \mathscr{C}_2 \Bigg[\left(\int_{t_{n-1}}^{t_n} \left\| \frac{\partial}{\partial t}(u - u_{h\tau}) \right\|_*^2 \mathrm{d}t \right)^{1/2} + \left(\int_{t_{n-1}}^{t_n} |||u - u_{h\tau}|||^2 \, \mathrm{d}t \right)^{1/2}$$

$$+ \left(\int_{t_{n-1}}^{t_n} \|\mathrm{div}(\mathbf{q}(u - u_{h\tau})\|^2 \, \mathrm{d}t \right)^{1/2} + \left(\int_{t_{n-1}}^{t_n} |\mathbf{G_h^n}(t)|^2 \, \mathrm{d}t \right)^{1/2}$$

$$+ \left(\int_{t_{n-1}}^{t_n} (|||u_h^{n-1} - u|||^2) \, \mathrm{d}t \right)^{1/2} + \|u_0\|_{0,\Omega} + \beta^{-1/2} \|f\|_{L^2(0,t_n;L^2(\Omega))} \Bigg]$$

for all $1 \leqslant n \leqslant N$.

Proof

Recall that for all $v \in H_0^1(\Omega)$ the term $A(v)$ is given by

$$A(v) = \sum_{V \in \mathscr{V}_h^n} \sum_{Q \subset V} \int_Q \mathbf{R_h^n}(v - I_m v) \, \mathrm{d}x + \sum_{E \in \mathscr{E}_h^n} \int_E \mathbf{r_h^n}(v - I_m v) \, \mathrm{d}s$$

$$- \sum_{\mathscr{T} \in \mathscr{T}_h^n} \sum_{\gamma_{ij} \in \Gamma_h^n, \gamma_{ij} \subset \mathscr{T}} ((I_m v)_i - (I_m v)_j) \int_{\gamma_{ij}} \mathbf{z_h^n} \, \mathrm{d}s \tag{42}$$

and has also the expression

$$A(v) = \sum_{\mathscr{T} \in \mathscr{T}_h^n} \int_T \mathbf{R_h^n} v \, \mathrm{d}x + \sum_{E \in \mathscr{E}_h^n} \int_E \mathbf{r_h^n} v \, \mathrm{d}s$$

Following [25, 26], we introduce for any element $\mathscr{T} \in \mathscr{T}_h^n$ and any edge $E \in \mathscr{E}_h^n$ the corresponding bubble functions ψ_K and ψ_E. We denote by ω_E the support of ψ_E which is the union of two

DOI: 10.1002/fld

elements of $\mathscr{T}_h^n$ sharing E and set

$$w_n = \delta_1 \sum_{\mathscr{T} \in \mathscr{T}_h^n} \alpha_T^2 \psi_T \mathbf{R_h^n} + \delta_2 D_{\min}^{-1/2} \sum_{E \in \mathscr{E}_h^n} \alpha_E \psi_E \mathbf{r_h^n}$$

Using the same arguments as in [26], we can choose the constants γ_1 and γ_2 such that

$$A(w_n) \geqslant (\eta_{\mathbf{R}}^n)^2 + (\eta_{\mathbf{r}}^n)^2 \tag{43}$$

$$|||w_n||| \leqslant C((\eta_{\mathbf{R}}^n)^2 + (\eta_{\mathbf{r}}^n)^2)^{1/2} \tag{44}$$

So we have

$$\begin{aligned} (\eta_{\mathbf{R}}^n)^2 + (\eta_{\mathbf{r}}^n)^2 + (\eta_z^n)^2 &= (\eta_h^n)^2 \leqslant A(w_n) + (\eta_z^n)^2 \\ |||w_n||| &\leqslant C^* \eta_h^n \end{aligned}$$

To bound the term η_h^n we use the last inequalities and (27). Let α be an arbitrary parameter such that $\alpha \geqslant 0$

$$\begin{aligned} \tau_n(\eta_h^n)^2 &= \int_{t_{n-1}}^{t_n} (\alpha+1) \left(\frac{t_n - t}{\tau_n}\right)^{\alpha} (\eta_h^n)^2 \,\mathrm{d}t \\ &\leqslant \int_{t_{n-1}}^{t_n} (\alpha+1) \left(\frac{t_n - t}{\tau_n}\right)^{\alpha} A(w_h) + \tau_n (\eta_z^n)^2 \,\mathrm{d}t \\ &\leqslant \int_{t_{n-1}}^{t_n} (\alpha+1) \left(\frac{t_n - t}{\tau_n}\right)^{\alpha} \int_\Omega \frac{\partial}{\partial t}(u - u_{h\tau}) w_n \,\mathrm{d}x \,\mathrm{d}t \\ &\quad + \int_{t_{n-1}}^{t_n} (\alpha+1) \left(\frac{t_n - t}{\tau_n}\right)^{\alpha} \int_\Omega D \nabla (u - u_{h\tau}) \cdot \nabla w_n \,\mathrm{d}x \,\mathrm{d}t \\ &\quad + \int_{t_{n-1}}^{t_n} (\alpha+1) \left(\frac{t_n - t}{\tau_n}\right)^{\alpha} \int_\Omega \mathrm{div}(\mathbf{q}(u - u_{h\tau})) w_n \,\mathrm{d}x \,\mathrm{d}t \\ &\quad + \int_{t_{n-1}}^{t_n} (\alpha+1) \left(\frac{t_n - t}{\tau_n}\right)^{\alpha} \int_\Omega a(u - u_{h\tau}) w_n \,\mathrm{d}x \,\mathrm{d}t \\ &\quad - \int_{t_{n-1}}^{t_n} (\alpha+1) \left(\frac{t_n - t}{\tau_n}\right)^{\alpha} (B(w_n) + C(w_n)) \,\mathrm{d}t + \tau_n (\eta_z^n)^2 \\ &\leqslant \int_{t_{n-1}}^{t_n} C^* \eta_h^n (\alpha+1) \left(\frac{t_n - t}{\tau_n}\right)^{\alpha} \left(\left\| \frac{\partial}{\partial t}(u - u_{h\tau}) \right\|_* + |||u - u_{h\tau}||| \right. \\ &\quad \left. + \beta^{-1/2} \| \mathrm{div}(\mathbf{q}(u - u_{h\tau})) \| + \mathscr{A} |||u - u_{h\tau}||| + \mathbf{G_h^n}(t) \right) \mathrm{d}t \\ &\quad - \int_{t_{n-1}}^{t_n} (\alpha+1) \left(\frac{t_n - t}{\tau_n}\right)^{\alpha} B(w_n) \,\mathrm{d}t + \tau_n (\eta_z^n)^2 \end{aligned}$$

DOI: 10.1002/fld

Since

$$\left(\int_{t_{n-1}}^{t_n}\left[(\alpha+1)\left(\frac{t_n-t}{\tau_n}\right)^{\alpha}\right]^2 \mathrm{d}t\right)^{1/2} = \tau_n^{1/2}\frac{\alpha+1}{\sqrt{2\alpha+1}}$$

we conclude that

$$\begin{aligned}\tau_n(\eta_h^n)^2 \leqslant\ & C^*\eta_h^n\tau_n^{1/2}\frac{\alpha+1}{\sqrt{2\alpha+1}}\left[\left(\int_{t_{n-1}}^{t_n}\left\|\frac{\partial}{\partial t}(u-u_{h\tau})\right\|_*^2 \mathrm{d}t\right)^{1/2}\right.\\ &\left.+(1+\mathscr{A})\left(\int_{t_{n-1}}^{t_n}|\!|\!|u-u_{h\tau}|\!|\!|^2\,\mathrm{d}t\right)^{1/2}+\beta^{-1/2}\left(\int_{t_{n-1}}^{t_n}\|\mathrm{div}(\mathbf{q}(u-u_{h\tau})\|^2\,\mathrm{d}t\right)^{1/2}\right]\\ &-\int_{t_{n-1}}^{t_n}(\alpha+1)\left(\frac{t_n-t}{\tau_n}\right)^{\alpha}B(w_n)\,\mathrm{d}t+\tau_n(\eta_z^n)^2\end{aligned}$$

Let us now bound the last integral in term of η_h^n. We have

$$\begin{aligned}\int_{t_{n-1}}^{t_n}(\alpha+1)\left(\frac{t_n-t}{\tau_n}\right)^{\alpha}B(w_n)\,\mathrm{d}t &= \tau_n\frac{\alpha+1}{\alpha+2}\int_\Omega (D_h^n\nabla(u_h^n-u_h^{n-1})\nabla w_n+a_h^n(u_h^n-u_h^{n-1})w_n)\,\mathrm{d}x\\ &\quad+\tau_n\frac{1}{\alpha+2}\int_\Omega \mathrm{div}(\mathbf{q}^{n-1}(u_h^n-u_h^{n-1}))w_n\,\mathrm{d}x\\ &\leqslant \tau_n^{1/2}\frac{\alpha+1}{\alpha+2}C_4(D,a,\beta)\sqrt{3}\boldsymbol{\Theta}_\mathbf{h}^\mathbf{n}C^*\eta_h^n\end{aligned}$$

Using Proposition 4.3 we obtain

$$\begin{aligned}\tau_n(\eta_h^n)^2 \leqslant\ & \mathscr{C}_3\tau_n^{1/2}\eta_h^n\left[\left(\int_{t_{n-1}}^{t_n}\left\|\frac{\partial}{\partial t}(u-u_{h\tau})\right\|_*^2 \mathrm{d}t\right)^{1/2}+\left(\int_{t_{n-1}}^{t_n}|\!|\!|u-u_{h\tau}|\!|\!|^2\,\mathrm{d}t\right)^{1/2}\right.\\ &\left.+\left(\int_{t_{n-1}}^{t_n}\|\mathrm{div}(\mathbf{q}(u-u_{h\tau})\|^2\,\mathrm{d}t\right)^{1/2}+\left(\int_{t_{n-1}}^{t_n}|\mathbf{G}_\mathbf{h}^\mathbf{n}(t)|^2\,\mathrm{d}t\right)^{1/2}\right]\\ &+\tau_n(\eta_h^n)^2C^*\mathscr{C}_1C_4\frac{\alpha+1}{\alpha+2}+\tau_n(\eta_z^n)(\eta_h^n)\end{aligned}$$

where $\mathscr{C}_3=\max((\alpha+1)/(\sqrt{2\alpha+1})\max(1+\mathscr{A},\beta^{-1/2}),(\alpha+1)/(\alpha+2)C_3\sqrt{3}\mathscr{C}_1)$.

Let $m\geqslant 1$ be an integer. Since $(\alpha+1)/(\alpha+2)\leqslant(\alpha+m)/(\alpha+2)$, we can choose α and m such that $C^*\mathscr{C}_1C_4(\alpha+1)/(\alpha+2)=\frac{1}{2}$ and conclude that

$$\begin{aligned}\tau_n^{1/2}\eta_h^n \leqslant\ & 2\mathscr{C}_3\left[\left(\int_{t_{n-1}}^{t_n}\left\|\frac{\partial}{\partial t}(u-u_{h\tau})\right\|_*^2 \mathrm{d}t\right)^{1/2}+\left(\int_{t_{n-1}}^{t_n}|\!|\!|u-u_{h\tau}|\!|\!|^2\,\mathrm{d}t\right)^{1/2}\right.\\ &\left.+\left(\int_{t_{n-1}}^{t_n}\|\mathrm{div}(\mathbf{q}(u-u_{h\tau})\|^2\,\mathrm{d}t\right)^{1/2}+\left(\int_{t_{n-1}}^{t_n}|\mathbf{G}_\mathbf{h}^\mathbf{n}(t)|^2\,\mathrm{d}t\right)^{1/2}\right]+2\tau_n^{1/2}\eta_z^n\end{aligned}$$

DOI: 10.1002/fld

Let us now bound the term $\tau_n^{1/2}\eta_z^n$. By (19), Lemma (4.2) and (7) we have

$$\begin{aligned}
(\tau_n^{1/2}\eta_z^n)^2 &= \int_{t_{n-1}}^{t_n} (\eta_z^n)^2\,\mathrm{d}t \\
&= \int_{t_{n-1}}^{t_n} D_{\min}^{-1/2} \sum_{\gamma_{ij}\subset\Gamma_h^n} \alpha_{\gamma_{ij}} \|\mathbf{q}^{n-1}\cdot\bar{\mathbf{n}}_{\gamma_{ij}}(u_h^{n-1}(x_i)-u_h^{n-1}(x)\|_{0,\gamma_{ij}}^2\,\mathrm{d}t \\
&\leqslant D_{\min}^{-1/2}\|\mathbf{q}\|_{(L^\infty(\Omega))^2} c_2 \int_{t_{n-1}}^{t_n} \sum_{\gamma_{ij}\subset\Gamma_h^n} \alpha_{\gamma_{ij}}^2 |||u_h^{n-1}|||_{\omega_{\gamma_{ij}}}^2\,\mathrm{d}t \\
&\leqslant D_{\min}^{-1/2}\|\mathbf{q}\|_{(L^\infty(\Omega))^2} 2c_2 \max_{\gamma\in\Gamma_h^n}\alpha_\gamma \int_{t_{n-1}}^{t_n} |||u_h^{n-1}|||^2\,\mathrm{d}t \\
&\leqslant D_{\min}^{-1/2}\|\mathbf{q}\|_{(L^\infty(\Omega))^2} 4c_2 \max_{\gamma\in\Gamma_h^n}\alpha_\gamma \int_{t_{n-1}}^{t_n} (|||u_h^{n-1}-u|||^2+|||u|||^2)\,\mathrm{d}t \\
&\leqslant \mathscr{C}_3 \int_{t_{n-1}}^{t_n} (|||u_h^{n-1}-u|||^2+\|u_0\|_{0,\Omega}^2+D_{\min}^{-1}\|f\|_{L^2(0,t_n;L^2(\Omega))}^2)\,\mathrm{d}t
\end{aligned}$$

where $\mathscr{C}_3 = D_{\min}^{-1/2}\|\mathbf{q}\|_{(L^\infty(\Omega))^2} 2c_2 \max_{\gamma\in\Gamma_h^n}\alpha_\gamma$. The result of Proposition 4.3 is proved by taking $\mathscr{C}_2=\max(\mathscr{C}_2,\mathscr{C}_3)$. □

5. NUMERICAL SIMULATIONS

In this section, we present some numerical results in 2-D based on the scheme presented in this paper for the concentration equation for miscible flow problems.

For the sake of completeness we recall the coupled system used for the simulations. The flow and transport of miscible displacement of one incompressible fluid by another through a porous medium Ω over a time period $]0,T[$ is governed by the following system (see, e.g. [18]):

Pressure equation:

$$\begin{aligned}
\mathbf{q} &= -\frac{K(x)}{\mu(c)}\nabla p \quad \text{in } \Omega\times]0,T[\\
\operatorname{div}\mathbf{q} &= 0 \quad \text{in } \Omega\times]0,T[
\end{aligned} \tag{45}$$

Concentration equation:

$$\Phi(x)\frac{\partial c}{\partial t} - \operatorname{div}(D(x,\mathbf{q})\nabla c - c\mathbf{q}) = f(x,t) \quad \text{in } \Omega\times]0,T[\tag{46}$$

subject to boundary and initial conditions, p and $\mathbf{q}$ are the pressure and Darcy velocity of the fluid mixture, Φ and K are the porosity and the permeability of the medium, μ is the viscosity of the mixture, c is the concentration of the contaminant solute, and f is the external flow rate.

DOI: 10.1002/fld

The form of the diffusion–dispersion tensor D that we use in our simulator is given by:

$$D(x,\mathbf{q}) = d_e I + |\mathbf{q}|[\alpha_l E(\mathbf{q}) + \alpha_t(I - E(\mathbf{q}))] \tag{47}$$

with $E_{ij}(\mathbf{q}) = q_i q_j/|\mathbf{q}|^2$, d_e is the effective diffusion coefficient, and α_l and α_t are the magnitudes of longitudinal and transverse dispersion, respectively.

Because the magnitude of the diffusion–dispersion tensor D is often much smaller than that of the Darcy velocity $\mathbf{q}$, the concentration equation (46) is a strongly convection–dominated PDE with small diffusion and dispersion terms indicated by the size of the coefficients d_e, α_l and α_t in (47). Moreover, (45)–(46) is a coupled system of PDEs which is typically defined on a very large physical domain.

One important issue in the simulation of porous medium flows is the manner in which the Darcy velocity $\mathbf{q}$ is calculated. Since the convection and diffusion–dispersion terms in (46) are governed by the Darcy velocity, accurate approximation of the concentration c requires an accurate approximation to the Darcy velocity $\mathbf{q}$.

An IMPES simulator, MFlow (cf. [32]), has been developed which applies a mixed hybrid finite element method [34] for computing an accurate approximation of the velocity $\mathbf{q}$ and the FV described here for the concentration equation. Our implementation for the test problems uses the lowest Raviart–Thomas element that specify piecewise constant pressure and piecewise continuous flux for the velocity.

It should be mentioned that the theoretical analysis of the method described in this paper for the coupled system is far from complete. Nevertheless the numerical experiments show, that with the FV discretization, the upwind and the adaptive grid control based on the error indicators, we have a powerful tool for solving flow and transport of miscible flow problems.

The two example problems used to illustrate the methodology are (1) a heterogeneous reservoir with two different permeability distributions, with values ranging from 10^{-5} to 1 and (2) the saltdome problem (cf. [8]). We begin the solution process with an initial coarse mesh which describes adequately the given problem (domain, coefficients, boundary conditions, and right-hand side). During the solution process the grid is refined (based on a criteria formulated from one of the three error estimators) until maximum refinement level is reached or the local error is found below a given threshold. The grids obtained from all error estimators differ slightly, but in all cases they are refined in the same areas and produce comparable results. In both cases, as expected, the meshes are refined around the areas where the singularities are located. The adaptivity of our FV method highly resolves the solution within the critical regions of the computational domain.

5.1. Test problem 1: heterogeneous case

In this example, we consider a heterogeneous reservoir $\Omega = (0,1)\times(0,1)$ with two different permeability distributions as shown in Figure 2: (black, $K = 10^{-5}$) and (white, $K = 1$). A source term is placed at the lower left-hand corner of the reservoir, Γ_{in}, and an outlet, Γ_{out}, is placed at the top right-hand corner of the reservoir. The boundary conditions are illustrated in Figure 2: $\mathbf{q}.\mathbf{n} = -0.1$ on Γ_{in} and $p = 1$ on Γ_{out}. All the Γ_{noflow} boundaries are no flow boundaries. The parameters were chosen as follows: $\Phi = 0.2$, $\mu = 1$, $d_e = 10^{-5}$, $\alpha_l = 5$, $\alpha_t = 0.5$, $c_0 = 0$ and $f = 1$ on Γ_{in} and $= 0$ elsewhere.

It is well known in literature that the jump of the coefficients at the inner boundaries may cause problems. We look for the behaviour of the adaptive algorithm near the inner boundaries.

DOI: 10.1002/fld

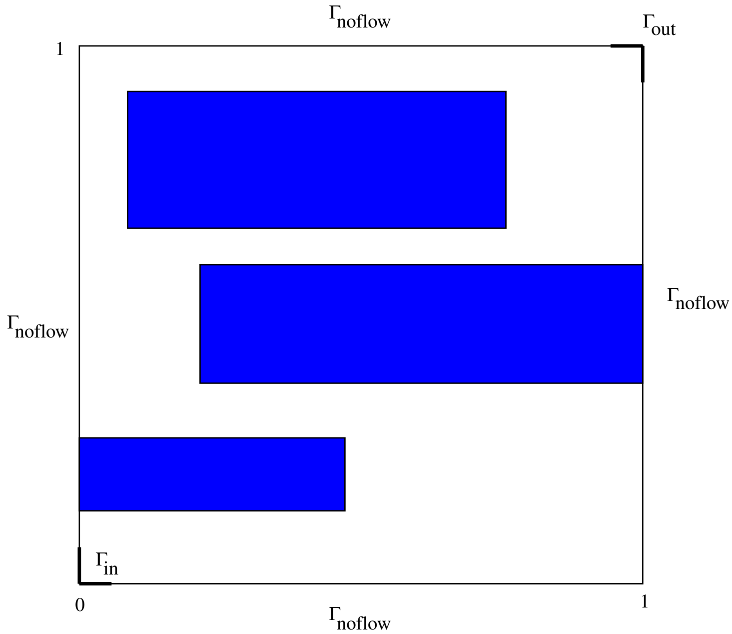

Figure 2. Permeability distribution and computational domain.

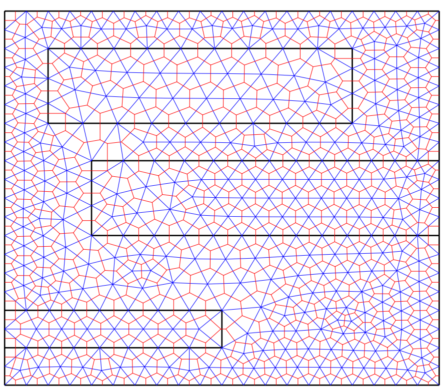

Figure 3. Primal grid.

In Figure 3 we present the primal grid and in Figure 4 the adaptive grid. From these figures, we can see that the local error estimators lead to local refinement around the expected regions where there are strong and sharp variation in permeability. Table I gives the results for the error indicators for different levels of refinement obtained. In order to compare these results with those when no local refinement is applied, we also include the computations obtained with a uniform grid (cf. Table I). We note that the grid follows the contour lines of the concentration as shown in Figure 6.

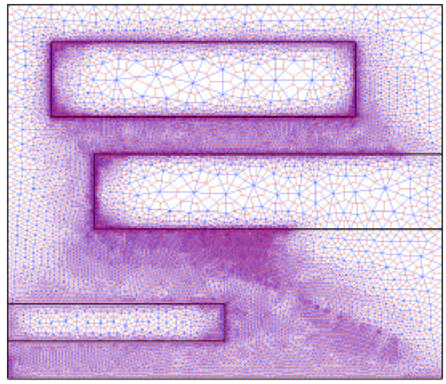

Figure 4. Adaptive grid.

Table I. Test problem 1 at $t=10$ years.

	Number of triangles	Level	CPU time	$\eta^n_{R_h}$	$\eta^n_{r_h}$	$\eta^n_{z_h}$
Primal grid	660	1	0 min 1.00 s	3.198e^{-02}	8.604e^{-07}	1.750e^{-02}
Adaptive grid	2885	2	0 min 20.81 s	8.26e^{-03}	3.655e^{-07}	1.281e^{-02}
	6424	3	0 min 48.18 s	4.359e^{-03}	6.521e^{-08}	1.042e^{-02}
	8894	4	1 min 10.55 s	2.940e^{-03}	4.623e^{-08}	9.794e^{-03}
	11 454	5	1 min 30.36 s	2.612e^{-03}	3.772e^{-08}	9.152e^{-03}
	14 562	6	1 min 59.53 s	2.413e^{-03}	3.371e^{-08}	8.341e^{-03}
	22 082	7	4 min 20.17 s	1.252e^{-03}	1.867e^{-08}	4.244e^{-03}
	27 382	8	5 min 59.17 s	1.023e^{-03}	1.012e^{-08}	3.152e^{-03}
Uniform grid	93 186	9	31 min 56.49 s	8.125e^{-04}	7.925e^{-09}	3.012e^{-03}

Moreover, at the inner boundaries of the domain the finer grid sizes appear. So the area, where we suppose the most problems in calculation, are of finer grid size. From concentration contours in Figures 5–7 and Table I, we can conclude that the accuracy of the solution obtained on a mesh with adaptive grid is comparable to the accuracy of the uniform grid, while the number of triangles are four times smaller.

5.2. *Test problem 2: saltdome*

We consider the saltdome problem presented in [8] which describes the flow over a saltdome which is sitting at the bottom of an aquifer initially filled with pure water ($c_0=0$). The computational domain is defined as $\Omega=[0,900]\times[0,300]$. The boundary and initial conditions are illustrated in Figure 8. At the top of the domain Ω a pressure difference is prescribed. The saltdome is situated in the middle of the lower boundary (see Figure 8). All other boundaries are no flow

DOI: 10.1002/fld

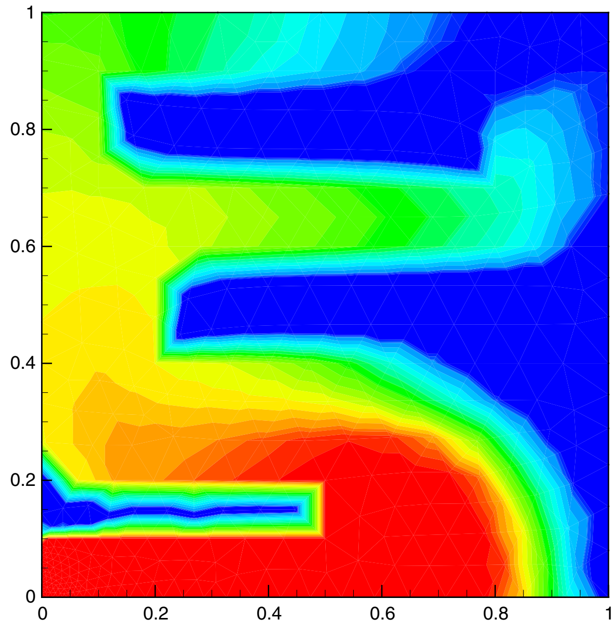

Figure 5. Concentration for primal grid.

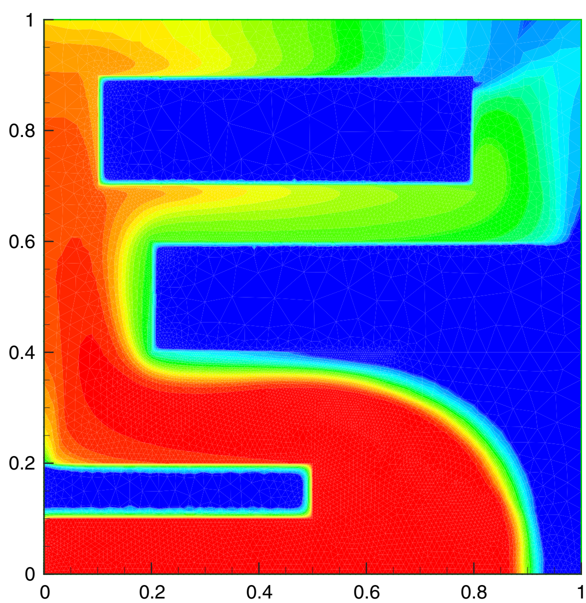

Figure 6. Concentration for adaptive grid.

DOI: 10.1002/fld

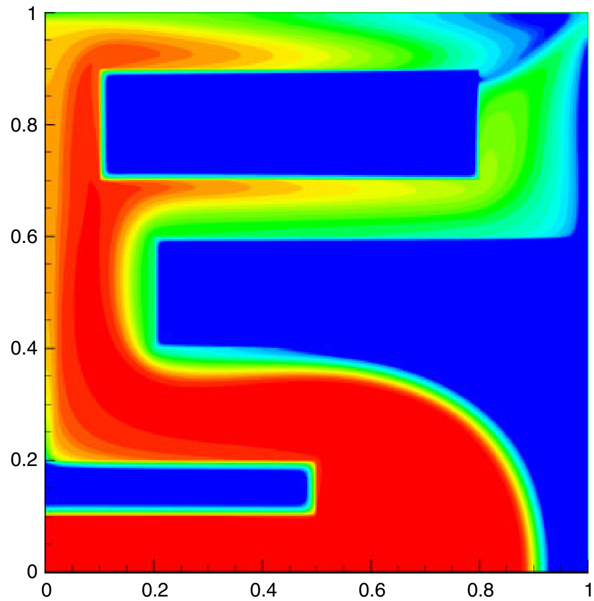

Figure 7. Concentration for uniform grid.

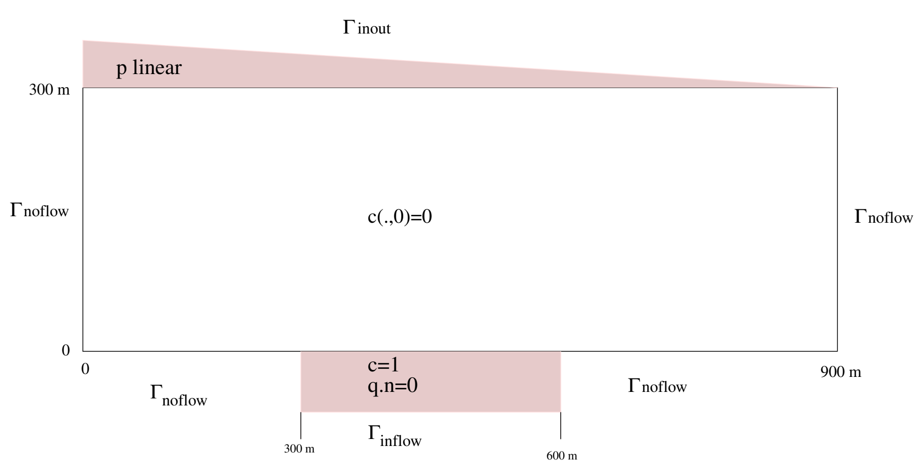

Figure 8. Geometry, initial and boundary conditions for the saltdome problem.

boundaries. The parameters were chosen as follows: $K=3.5\times 10^{-2}$, $\Phi=0.2$, $d_{\mathrm{e}}=0.86$, $\mu=1$, $\alpha_{\mathrm{l}}=20$, $\alpha_{\mathrm{t}}=2$, and $p=-111x+10^5$ at the top boundary. Here the singularity is due to the source term, which is taken to be 1 concentrated at the boundary Γ_{inflow} (see Figure 8). Figures 9–11 show the adaptive grid and the salt concentration at three time steps. Table II gives the results for the error indicators for different levels of refinement and the computations obtained

DOI: 10.1002/fld

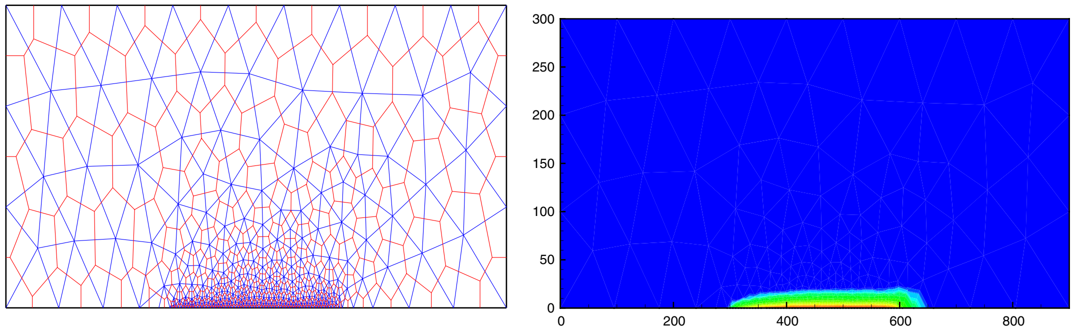

Figure 9. Adaptive grid and concentration contours at $t = 5$ years.

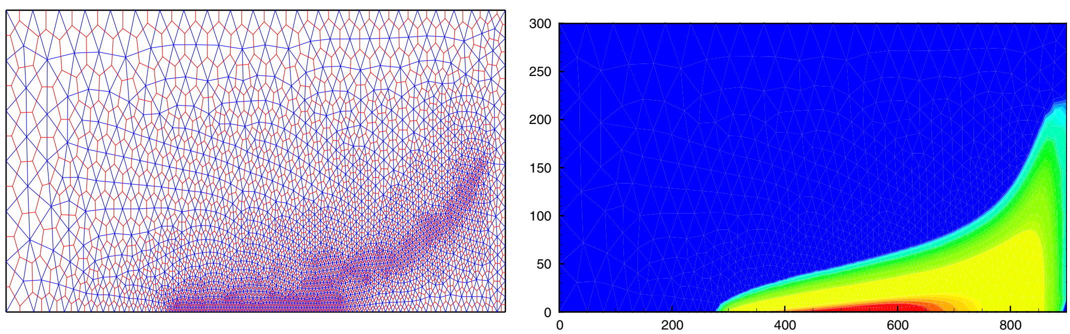

Figure 10. Adaptive grid and concentration contours at $t = 40$ years.

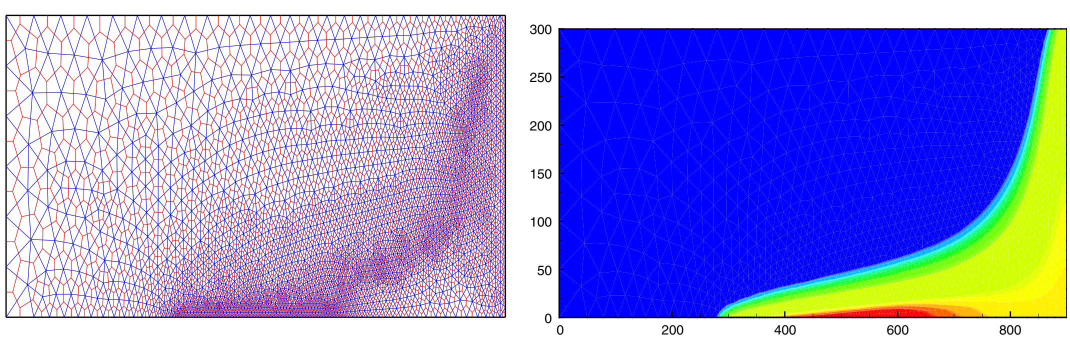

Figure 11. Adaptive grid and concentration contours at $t = 240$ years.

with a uniform grid. Again, we can see that the local error estimators lead to local refinement around the expected concentration front. The salt concentration shows good agreement with those in [8].

DOI: 10.1002/fld

Table II. Test problem 2.

	Number of triangles	Level	CPU time	$\eta^n_{R_h}$	$\eta^n_{r_h}$	$\eta^n_{z_h}$	Final time (years)
Mesh 0	505	1	0 min 0.12 s	$2.246e^{-02}$	$1.377e^{-02}$	$3.637e^{-03}$	5
	779	2	0 min 0.25 s	$7.027e^{-03}$	$1.157e^{-02}$	$3.041e^{-03}$	
Mesh 1	2710	1	0 min 1.91 s	$5.493e^{-03}$	$9.983e^{-03}$	$3.827e^{-03}$	40
	3591	2	0 min 2.71 s	$5.041e^{-03}$	$8.950e^{-03}$	$3.410e^{-03}$	
Mesh 2	3400	1	0 min 10.50 s	$4.576e^{-03}$	$8.412e^{-03}$	$3.640e^{-03}$	240
	5552	2	0 min 35.48 s	$1.788e^{-03}$	$8.388e^{-03}$	$3.274e^{-03}$	
	8582	3	1 min 14.99 s	$1.423e^{-03}$	$7.647e^{-03}$	$2.914e^{-03}$	
	11 068	4	1 min 42.31 s	$3.618e^{-04}$	$6.624e^{-03}$	$2.304e^{-03}$	
	19 045	5	8 min 0.63 s	$4.323e^{-05}$	$1.361e^{-03}$	$1.250e^{-03}$	
Uniform grid	41 318	6	28 min 7.51 s	$1.922e^{-05}$	$8.910e^{-04}$	$7.420e^{-04}$	240

ACKNOWLEDGEMENTS

The work of B. Amaziane was partially supported by the GdR MoMaS 2439 CNRS ANDRA BRGM CEA EDF IRSN whose support is gratefully acknowledged. This work was partially supported by the CMIMF Actions Intégrées N^0 $MA/02/34$ and $MA/04/94$ whose support is gratefully acknowledged. The authors gratefully thank the anonymous referees for their insightful comments and suggestions.

REFERENCES

1. Barth T, Ohlberger M. Finite volume methods: foundation and analysis. In *Encyclopedia of Computational Mechanics*, Stein E, de Borst R, Hughes TJR (eds). Wiley: New York, 2004.
2. Eymard R, Gallouët T, Herbin R. The finite volume method. In *Handbook of Numerical Analysis*, Ciarlet PG, Lions JL (eds). North-Holland: Amsterdam, 2000; 715–1022.
3. Feistauer M, Felcman J, Straskraba I. *Mathematical and Computational Methods for Compressible Flow*. Oxford Sciences Publications: Oxford, 2003.
4. Herbin R, Kröner D (eds). *Finite Volumes for Complex Applications III*. Hermes Penton Science: London, 2002.
5. Kröner D. *Numerical Schemes for Conservation Laws*. Wiley-Teubner: Stuttgart, 1997.
6. LeVeque RJ. *Finite Volume Methods for Hyperbolic Problems*. Cambridge University Press: New York, 2002.
7. Li RH, Chen ZY, Wu W. *Generalized Difference Methods for Differential Equations*. Marcel Dekker: New York, 2000.
8. Bürkle D, Ohlberger M. Adaptive finite volume methods for displacement problems in porous media. *Computing and Visualization in Science* 2002; **5**(2):95–106.
9. Coudière Y, Gallouët T, Herbin R. Discrete Sobolev inequalities and L^p error estimates for finite volume solutions of convection diffusion equations. *M2AN, Mathematical Modelling and Numerical Analysis* 2001; **35**(4):767–778.
10. Herbin R. An error estimate for a finite volume scheme for a diffusion–convection problem on a triangular mesh. *Numerical Methods for Partial Differential Equations* 1995; **11**(2):165–173.
11. Lazarov R, Mishev ID, Vassilevski PS. Finite volume methods for convection–diffusion problems. *SIAM Journal on Numerical Analysis* 1996; **33**(1):31–55.
12. Lazarov R, Tomov S. A posteriori error estimates for finite volume element approximations of convection–diffusion-reaction equations. *Computational Geosciences* 2002; **6**(3–4):483–503.
13. Michel M. A finite volume scheme for two-phase immiscible flow in porous media. *SIAM Journal on Numerical Analysis* 2003; **41**(4):1301–1317.
14. Morton KW. *Numerical Solution of Convection–Diffusion Problems*. Chapman & Hall: London, 1996.

15. Morton KW, Stynes M, Süli E. Analysis of a cell-vertex finite volume method for convection–diffusion problems. *Mathematics of Computation* 1997; **66**(220):1389–1406.
16. Ohlberger M, Rohde C. Adaptive finite volume approximations for weakly coupled convection dominated parabolic systems. *IMA Journal on Numerical Analysis* 2002; **22**(2):253–280.
17. Wang S, Sun S. The characteristic finite volume method for nonlinear convection–diffusion problems. *Northeastern Mathematics Journal* 1999; **15**(4):408–422.
18. Bear J, Bachmat Y. *Introduction to Modeling of Transport Phenomena in Porous Media*. Kluwer Academic Publishers: Dordrecht, 1991.
19. Ainsworth M, Oden JT. *A Posteriori Error Estimation in Finite Element Analysis*. Wiley: Chichester, 2000.
20. Verfürth R. *A Review of a Posteriori Error Estimation and Adaptive Mesh-Refinement Techniques*. Teubner-Wiley: Stuttgart, 1996.
21. Ohlberger M. A posteriori error estimates for vertex centred finite volume approximations of convection–diffusion-reaction equation. *M2AN*, *Mathematical Modelling and Numerical Analysis* 2001; **35**:355–387.
22. Afif M, Bergam A, Mghazli Z, Verfürth R. *A posteriori* estimators for the finite volumes discretization of an elliptic problem. *Numerical Algorithms* 2003; **34**:127–136.
23. Bergam A, Mghazli Z. Estimateurs *a posteriori* d'un schéma de volumes finis pour un problème non linéaire. *Comptes Rendus de l'Académie des Sciences* 2000; **331**(6):475–478.
24. Bergam A, Mghazli Z, Verfürth R. Estimations *a posteriori* d'un schéma de volumes finis pour un problème non Linéaire. *Numerische Mathematik* 2003; **95**:599–624.
25. Verfürth R. *A posteriori* error estimates for finite element discretizations of the heat equation. *Calcolo* 2003; **40**:195–212.
26. Verfürth R. Robust *a posteriori* error estimates for nonstationary convection–diffusion equations. *SIAM Journal on Numerical Analysis* 2005; **43**(4):1783–1802.
27. Dautray R, Lions JL. *Mathematical Analysis and Numerical Methods for Science and Technology*. Springer: Berlin, 1992.
28. Ciarlet PG. *The Finite Element Method for Elliptic Problems*. North-Holland: Amsterdam, 1978.
29. Afif M, Amaziane B. Convergence of finite volume schemes for a degenerate convection–diffusion equation arising in flow in porous media. *Computer Methods in Applied Mechanics and Engineering* 2002; **191**:5265–5286.
30. Afif M, Amaziane B. Numerical simulation of two-phase flow through heterogeneous porous media. *Numerical Algorithms* 2003; **34**:117–125.
31. Amaziane B, El Ossmani M. Convergence analysis of an approximation to miscible fluid flows in porous media by combining mixed finite element and finite volume methods, Preprint, 2005. http://lma.univ-pau.fr/data/pub/pub_pdf2005/0505.pdf
32. Amaziane B, El Ossmani M, Serres C. Numerical modelling of the flow and transport of radionuclides in heterogeneous porous media. *Computational Geosciences* 2007, to appear.
33. Verfürth R. *A posteriori* error estimations for convection–diffusion equations. *Numerische Mathematik* 1998; **80**:641–663.
34. Brezzi F, Fortin M. *Mixed and Hybrid Finite Element Methods*. Springer: New York, 1991.

DOI: 10.1002/fld